Shahrood University of Technology

Journal of Mining and Environment (JME)

Journal homepage: www.jme.shahroodut.ac.ir

Iranian Society of Mining Engineering (IRSME)

Prediction and Optimization of Ground Vibration Caused by Blasts Using a Combination of Statistical Models and FROG Algorithm (Case Study: Gol-e-Gohar Iron Ore Mine No. 1)

Abbas Khajouei Sirjani[1*], Farhang Sereshki[1], Mohammad Ataei[1], and Mohammad Amiri Hosseini[2]

1. Faculty of Mining, Petroleum & Geophysics Eng., Shahrood University of Technology, Shahrood, Iran
2. The Department of Mining and Geology of Research and Technology Management of Gol-e-Gohar, Sirjan, Iran

Article Info

Received 9 July 2024
Received in Revised form 10 September 2024
Accepted 18 November 2024
Published online 18 November 2024

DOI: 10.22044/jme.2024.14747.2793

Keywords

Blasting
Ground Vibration
Statistical Models
Frog Algorithm
Gol-e-Gohar Mine

Abstract

The most significant detrimental consequence of blasting operations is ground vibration. This phenomenon not only causes instability in the mine walls but also extends its destructive effects to various facilities and structures over several kilometers. Various researchers have proposed equations for predicting Peak Particle Velocity (PPV), which are typically based on two parameters: the charge per delay and the distance to the blast site. However, according to different studies, the results of blasting operations are influenced by several factors, including the blast pattern, rock mass properties, and the type of explosives used. Since artificial intelligence technology has not yet been fully assessed in the mining industry, this study employs linear and nonlinear statistical models to estimate PPV at Golgohar Iron Ore Mine No. 1. To achieve this goal, 58 sets of blasting data were collected and analyzed, including parameters such as blast hole length, burden thickness, row spacing of the blast holes, stemming length, the number of blast holes, total explosive charge, the seismograph's distance from the blast site, and the PPV recorded by an explosive system using a detonating fuse. In the first stage, ground vibration was predicted using linear and nonlinear multivariate statistical models. In the second stage, to determine the objective function for optimizing the blast design using the shuffled frog-leaping algorithm, the performance of the statistical models was evaluated using R^2, RMSE, and MAPE indices. The multivariate linear statistical model, with $R^2 = 0.9247$, RMSE = 9.235, and MAPE = 12.525, was proposed and used as the objective function. Ultimately, the results showed that the combination of the statistical model technique with the shuffled frog-leaping algorithm could reduce PPV by up to 31%.

1. Introduction

Blasting has been used as one of the most effective techniques in recent decades for breaking rocks in civil and mining projects. When explosive material detonates inside a blast hole, a significant amount of energy is transferred as a shockwave the ground, and gases are released into the air [1]. Approximately 30 to 35 percent of the energy generated by blasting is used for breaking and displacing rocks, while the remaining energy is lost through ground vibration, air blast, and rock ejection [2]. Numerous studies have been conducted to examine the factors influencing ground vibration caused by blasts. Yu Yang and Xiaoming Hu investigated the parameters affecting ground vibration from blasts. Research has shown that the maximum charge per delay, the distance from the blast source to observation points, and geological conditions are fundamental factors in predicting ground vibration [3]. Arthur developed a novel method for predicting ground vibration resulting from blasts using Gaussian Process Regression (GPR) [4]. Li used experimental methods and artificial intelligence (AI) approaches to determine the maximum particle velocity. The correlation coefficients for these models were 0.799, 0.747, and 0.724, respectively.

Corresponding author: abbas3457@gmail.com (A. Khajouei Sirjani)

Subsequently, predictions obtained using AI methods had higher correlation coefficients and demonstrated better predictive capabilities compared to those derived from experimental methods [5]. Khandelwal and Singh investigated empirical relationships for estimating ground vibration and then compared their results using an artificial neural network. The findings indicate that a neural network can be an effective tool for estimating ground vibration resulting from blasts [6]. Singh and Roy examined the effects of ground vibration on buildings and structures in the blast area. According to their research, single-story concrete structures exhibit the highest resistance to ground vibration [7]. Dehghani and Ataiepour used neural networks to assess the importance of each parameter affecting ground vibration. They subsequently developed a dimensional analysis relationship for measuring ground vibration using an empirical method [8]. Manjazi et al. used a neural network as a research tool in their study on ground vibration at the Golgohar mine. The results indicate that two parameters, specifically the specific charge and maximum charge, are among the most important factors required for predicting ground vibration using empirical models [9]. Hasani Panah et al. employed multiple regression and empirical models to predict ground vibration in the Miduk copper mine [10]. Shirani and Manjazi, in their research at the Golgohar mine, aimed to predict and minimize ground vibration using the GEP and COA algorithms [11]. Regam and Nima Jah investigated ground vibration in an iron ore mine in India using artificial neural networks [12]. Ataie and Sarcheki examined ground vibration in limestone rocks using a genetic algorithm [13]. Various researchers have employed a range of metaheuristic algorithms to evaluate influential parameters, predict Peak Particle Velocity (PPV), and analyze damages resulting from blasting operations. These algorithms include neural networks, genetic algorithms, ant colony optimization algorithms, random decision trees, particle swarm optimization, support vector machines, and numerical simulation approaches [14-28]. Table 1 shows recent studies on the use of different models to predict blast-induced Peak Particle Velocity (PPV).

Table 1. Some studies have predicted PPV based on various models

Reference	year	Authors	Input variables	Output	No. of dataset	Models	Performance Indices The best model
[29]	2024	Zhao et al	Qmax,Qtotal D, VD, B, PPR, DT RMI, f α, VoD	PPV	180	CGO-ANN GA-ANN PSO-ANN Single ANN USBM	CGO-ANN: R-squared=0.909 MAE=0.425 RMSE=0.508 MSE=0.259
[30]	2023	Fissha et al	MIC, SD DIS,E,BlO Bla,MlO Mla	PPV	100	BNN, GBR KNR, DTR RFR	BNN R-squared=0.94 MSE=0.03 RMSE=0.17
[31]	2023	Guo et al	W, R, H B, S, H_0, PF	PPV	50	PSO-LSSVM LSSVM GA-BP, BP	PSO-LSSVM: R-squared=0.965 MAE=1.717 RMSE=1.954
[32]	2023	Keshtegar et al	Mc, B/S, St E, Vp, Di	PPV	90	RSM-SVR PSO-SVR GA-SVR MLR SVR, RSM	RSM-SVR: R-squared=0.896 MAE=1.379 RMSE=1.619 NSE=0.686 d=0.832
[33]	2023	Fissha et al	N, B/D_e H/B, Q D, S, B	PPV	140	GPR, DT SVR	GPR: R-squared=0.94 MSE=0.001 MAE=0.026 RMSE=0.038
[34]	2023	Armaghani et al	C, DIS	PPV	154	ANN Neuro-Swarm Neuro-Imperialism	Neuro-Swarm: R-squared=0.85 MAE=1.17 RMSE=0.075 VAF (%) =90.606 a20−index=0.35
[35]	2022	Bhatawdekar et al	AD, B, S DIS, PF S, T, MC	PPV	101	GPR, BPNN ELM, MARS MVRA	GPR: R-squared=0.99 MSE=0.0903 R=0.9985 VAF (%) = 99.172
[36]	2022	He et al	BS, HD, ST, PF, MCDIS	PPV	102	FR-WOA FR-GWO FR-TSA	FR-WOA: Rsquared = 0.932 MAE=0.188 RMSE=0.246 VAF (%) = 95.032
[37]	2021	Lawal et al	DIS,W,ρ SRH	PPV	100	GEP, ANFIS SCA-ANN	SCA-ANN: R-squared = 0.99

Table 1. Cont

Reference	year	Authors	Input variables	Output	No. of dataset	Models	Performance Indices The best model
[38]	2021	Jelušič et al	Q, DIS	PPV	40	ANFIS	R-squared=0.87 Adjusted R-squared = 0.84 SSE=4.67 RMSE = 0.88
[39]	2021	Srivastava et al	B, S, HD CH-H, CH-R, ST N-BH, PF Qmax,DIS	PPV	73	RF, SVM	RF: R-squared=0.81SV: R-squared=0.75
[40]	2020	Pantachang et al	SD, DIS, AC	PPV	-	FS	-
[41]	2020	Lawal & Adebayo Idrisa	PF, W, DIS	PPV	88	ANN	R-squared=1
[42]	2020	Yu et al	f, Qmax Qtotal,T B, DH, DV	PPV	137	HHO-RF	R-squared=0.94 MAE=0.29 RMSE=0.34
[43]	2020	Zhang et al	BS, DIS ST, MC PF, HD	PPV	102	RF, CART CHAID ANN, SVM	SVM: R-squared = 0.85 MAE = 1.17 RMSE = 1.5 VAF (%) = 84.54
[44]	2020	Mahdiyar et al	ST, BS, C PF, D	PPV	149	GEP	R-squared=0.68 RMSE=4.0344
[45]	2020	Li et al	B, S, ST PF, W RMR, D	PPV	80	BBO-ANN PSO-ANN MPMR, ELM DIRECTANN USBM IndianStandard Ambraseys – Hendron	BBO-ANN: R-squared=0.988 MAE=0.022 RMSE=0.026 RSR=0.109 d=0.997
[46]	2020	Shakeri et al	CHD DIS, B, S, SP	PPV	113	LMR,ANNs,GEP	GEP: R-squared=0.91 RMSE=2.67
[47]	2020	Mohammadi et al	HD, NH S, B, Q	PPV	45	ICA Kmeans,TOPSIS	-
[48]	2018	Ragama& Nimajeb	Q, DIS	PPV	14	GRNN	R-squared=0.998 MSE=0.0001

2. Case Study Introduction and Data Collection

The Gol-e-Gohar iron ore mines consist of six anomalies located in the Kerman province, 55 kilometers southwest of Sirjan, 235 kilometers from the center of the province, and 320 kilometers southeast of Shiraz. Iron Ore Mine No. 1 at Golgohar has geological reserves of approximately 313 million tons, most of which are economically extractable. The general shape of the No. 1 reserve is roughly elongated in the NW-SE direction. In Figure 1, the location of the Golgohar Iron Ore Mine No. 1 anomaly relative to other anomalies in the Golgohar complex, transportation routes, and satellite imagery illustrates the study area's position. The mining method in the study mine is open-pit, and various mining operations are carried out simultaneously by drilling and blasting operations to obtain suitable feed for transport to the processing plant. The rock units in this mine include Paleozoic metamorphic rocks, Mesozoic and Cenozoic sedimentary rocks, and Quaternary sediments. Drilling and blasting operations at the Golgohar Iron Mine Number One are carried out in a network of grids using various machines. The diameter of the blast holes is determined based on the type of rock, generally using diameters of 6 and 8 inches for iron ore and 8 and 10 inches for overburden. The explosive used in the mine is ANFO to a depth where groundwater does not pose a problem, and beyond that, suitable explosives like Emulsifier are used. The design of blasting blocks is carried out by experts using Gemcom software, taking into account the type of rock, bench height, and drill bit diameter. For iron ore blasting blocks, experts use a pattern of 3×4 meters for 6-inch diameters and 4×5 meters for 10-inch diameters. For overburden and waste rock blasting blocks, a 7×9 meter pattern is typically considered for 10-inch diameters.

In this study, ground vibrations resulting from 58 blasts in the northern, northeastern, and eastern parts of the mine were evaluated using the BMIII seismograph manufactured by Instantel Canada, of the BLAST MATE III type. Figure 2 illustrates the peripheral equipment and the installation procedure of the seismograph. Subsequently, information related to the geometric parameters of blast patterns such as blast hole length, burden, spacing, stemming length, and the number of blast holes drilled in each blast block was separately measured for each blast. Tables 2 and 3 present the descriptive statistical analysis and the examination of parameters using Pearson correlation coefficients for the dataset. Figure 3 illustrates the

histogram of the frequency distribution of the input and output parameters. Pearson's correlation coefficient is a statistical tool used to determine the type and degree of relationship between two quantitative variables. The coefficient indicates the strength and type (direct or inverse) of the relationship. The range of this coefficient is between -1 and 1, and if the correlation coefficient equals zero, it indicates no relationship between the two variables. A positive correlation coefficient indicates an approximate direct relationship between the two variables, while a negative coefficient indicates an approximate inverse relationship. The greater the absolute value of the correlation coefficient, the stronger the relationship between the two variables.

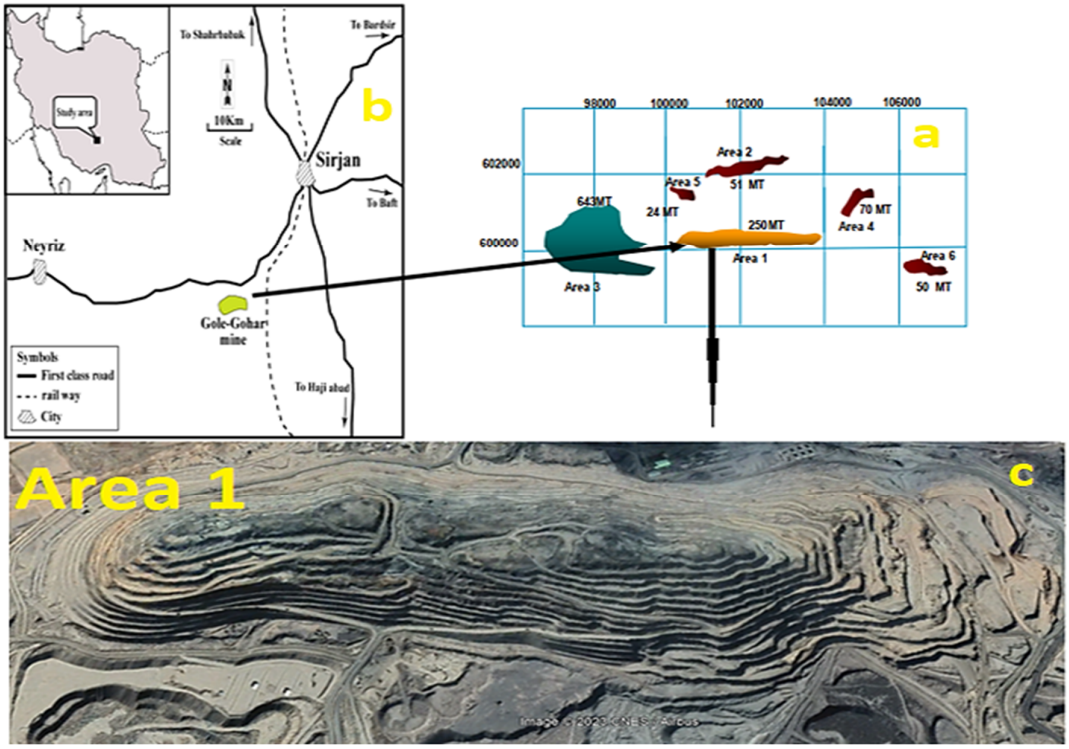

Figure 1. a) Location of the anomaly, b) Location of transportation routes, and c) Satellite image of Gol-e-gohar Mine No. 1

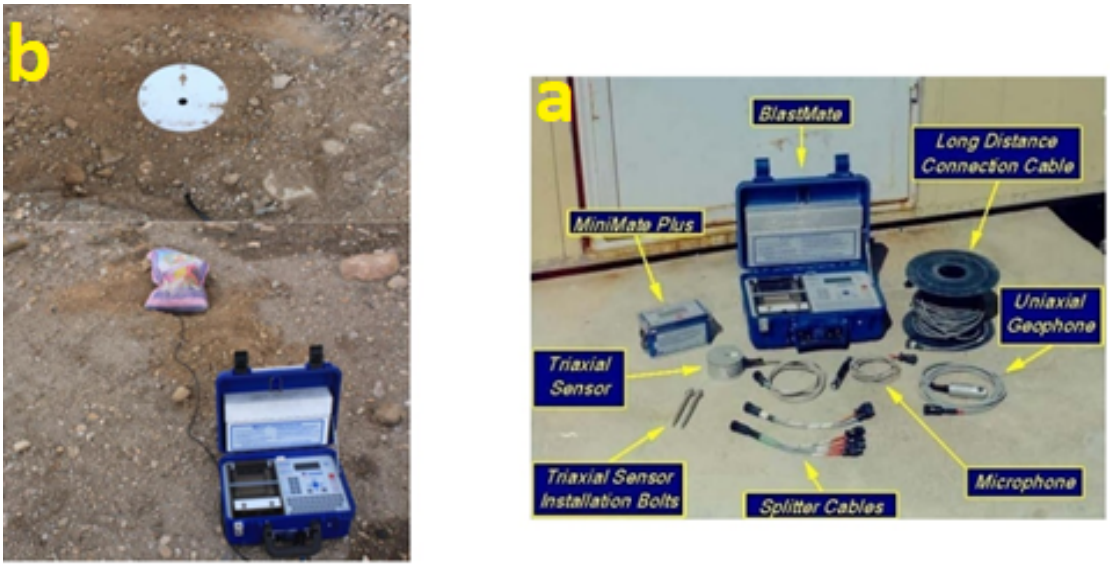

Figure 2. a) BLAST MATE III seismograph and its peripheral equipment, b) Procedure of placement of the sensor on the ground

Table 2. Descriptive statistics of collected data related to the geometric parameters of blasting patterns

Parameter	Variable category	Symbol	Min	Mean	Max	Std.Error of Mean	Std. Deviation
ole-depth (m)	Input	H	6.8	12.195	17.5	0.4086	2.5842
Burden(m)		B	2.8	5.565	7.5	0.2328	1.4722
Spacing (m)		S	4	6.908	9.5	0.2706	1.7114
Stemming (m)		ST	2.5	4.165	6	0.1408	0.8906
No. of holes		N.H	21	43.75	77	2.577	16.297
Total charge (kg)		Q	6400	20716.5	33250	1210.3	7654.63
Distance (m)		DIS	62	122.13	188	5.687	35.966
PPV (mm/s)	Output	PPV	12	66.28	136	5.125	32.416

Table 3. Pearson correlation coefficient matrix related to the geometric parameters of blast patterns

Parameter	H	B	S	ST	N	Q	DIS	PPV
Hole depth	1							
Burden	0.816	1						
Spacing	0.796	0.935	1					
Stemming	0.985	0.804	0.777	1				
No. of holes	0.870	0.807	0.818	0.875	1			
Total charge	0.855	0.892	0.867	0.860	0.902	1		
Distance	0.843	0.921	0.891	0.834	0.833	0.879	1	
PPV	0.876	0.889	0.890	0.868	0.901	0.909	0.918	1

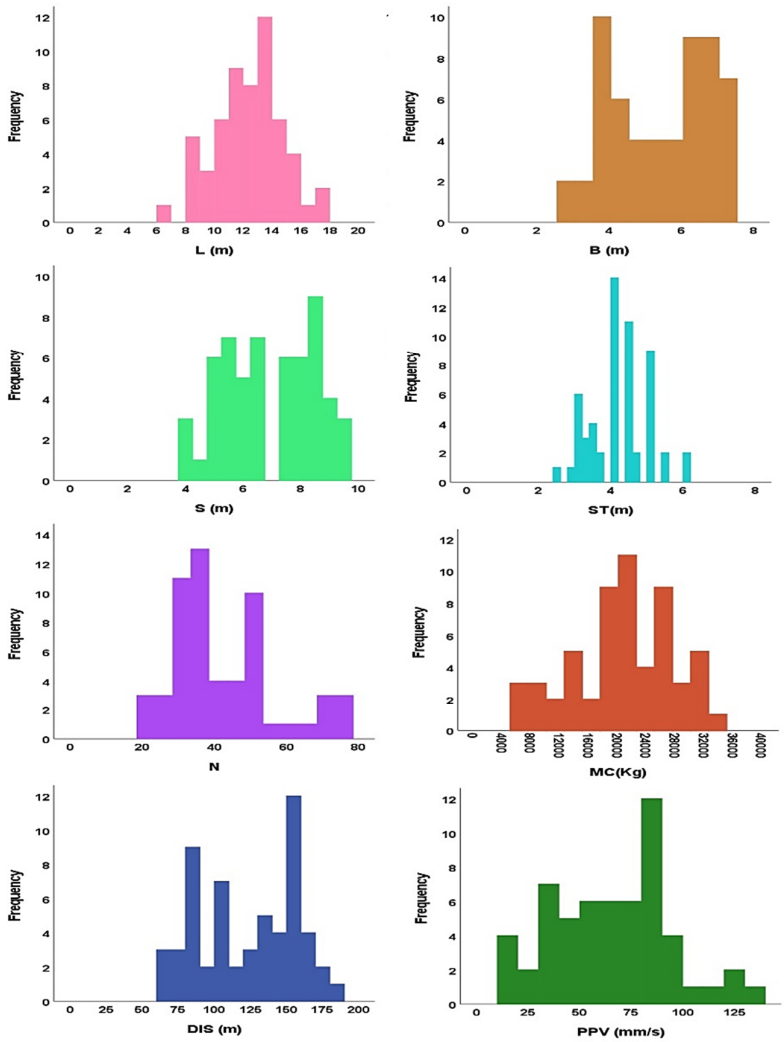

Figure 3. Histogram of the frequency distribution of input and output parameters.

3. Methodology

3.1. Statistical models

Multiple Statistical Models, due to their high interpretability and precise generalization, have become one of the main tools for problem-solving in various engineering fields. Linear and nonlinear multiple regression models demonstrate the influence of multiple variables on a dependent variable [49, 50].

3.2. Frog Leap Algorithm

The Shuffled Frog Leap Algorithm is one of the comprehensive optimization algorithms first introduced in 2003 by Eusuff et al. [51]. The SFLA algorithm is inspired by the social behavior of frogs in searching for food resources. It is an evolved version of the Stochastic Evolution Communities (SCE) algorithm, incorporating elitism and collective intelligence, resulting in the Frog Leap Algorithm [52]. SFLA is a combination of Genetic Algorithms (GA) and Particle Swarm Optimization (PSO), designed based on their behavioral patterns [53]. In this algorithm, each frog has a chromosome-like structure. The entire frog population is divided into smaller subgroups so that these subgroups can conduct searches in their local environments. Each subgroup of frogs has a representative of different types of frogs scattered in different environments [54, 55]. On the other hand, each frog within each subgroup is influenced by its group members and other groups. After several stages, information and messages, along with local and global searches, continue until convergence criteria are met [56]. The SFLA algorithm demonstrates high capability in global search and can solve various problems, including linear, nonlinear, mixed-integer, and various other optimization problems. An overview of the Frog Leap Algorithm process is presented in Figure 4. In this algorithm, the initial population of frogs is generated randomly within the defined ranges for the problem, as shown in Equation (1).

$$X_i = X_i^i + \alpha(X_i^h - X_i^i) \quad (1)$$

In this context, X_i represents the position of each member of the population, X_i^i the lower bound, X_i^h the upper bound, and α a random value between 0 and 1. Each frog represents a valid solution to the optimization problem, and it has a specific fitness value. The frogs are sorted in descending order based on their fitness values, and then they are divided into several different categories. If the initial population consists of P frogs and is divided into m groups, the frogs are divided into these groups based on the objective function. After sorting, the first frog is placed in the first group, the second frog in the second group, the third frog in the third group, and so on, with frog m + 1 placed in the first group. In the end, each of the m groups will contain n members [57, 58], according to Relation (2).

$$P = m \times n \quad (2)$$

In each set, the position of the i-th frog, denoted by X_g, is determined based on the difference between the frog with the best fitness, represented by X_b, and the frog with the worst fitness, represented by X_w, using Equation (3).

$$X_g = \alpha(X_b - X_w) \quad (3)$$

Equation (3) calculates the difference between the fitness of different frogs in the set. The new position of the frog is obtained using Equation (4), which D_{max} represents the maximum changes that can be applied to the frog position. Then the position of the frog is improved using the following relationship according to Figure 5.

$$X_w = P_c X_w + X_g$$
$$D_{max} \le X_g \le -D_{max} \quad (4)$$

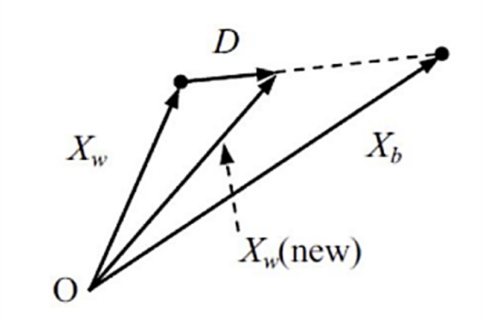

Figure 5. Frog Position Improvement

If this change in position leads to the generation of frogs with better fitness, these frogs will replace the unfit frogs. Otherwise, a frog with superior fitness in the entire population X_g will replace X_b in Equation (3), and a new frog will be generated. This process will continue until complete convergence is achieved or one of the stopping criteria is met.

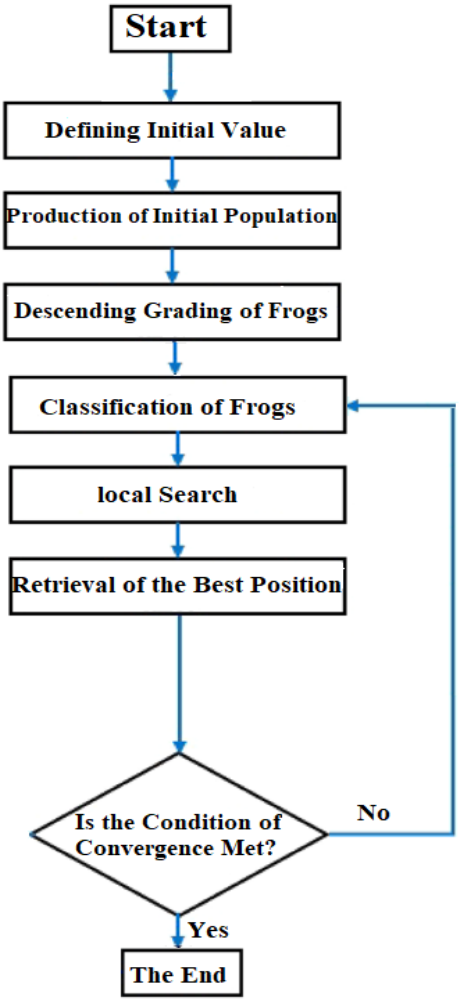

Figure 4. Overview of the Frog Leaping Algorithm Process

4. Modeling and Predicting PPV Using Statistical Models

In this study, the aim is to build multivariable linear and nonlinear statistical models to predict PPV to select the best model to optimize the blast pattern in the SPSS27 software environment. Initially, for model construction, 70% of all data were randomly used for model training, and the remaining 30% were used for model testing. Linear, logarithmic, exponential, and polynomial statistical models with non-linear coefficients were constructed to predict PPV according to equations (5 to 8).

$$PPV = -45.212 + 1.905(L) - 0.697(B) + 3.633(S) - 1.1(ST) + 0.524(N) + 0.001(MC) + 0303(DIS) \quad (5)$$

$$PPV = EXP[-0.442 + 0.183(L)^{0.505} + 0.001(B)^{0.326} + 0.000005(S)^{0.328} + 0.008(ST)^{0.219} + 0.001(N)^{0.463} + 0.219(MC)^{-0.673} + 0.059(DIS)^{0.39}] \quad (6)$$

$$PPV = [-313.199 + 22.983\ln(L) + 9.79\ln(B) + 26.592\ln(S) - 5.65\ln(ST) + 38.997\ln(N) - 1.113\ln(MC) + 34.149\ln(DIS)] \quad (7)$$

$$PPV = [-0.008 + 0.098(L)^{0.106} + 0.161(B)^{0.253} + 0.147(S)^{0.209} + 0.18(ST)^{0.243} + 0.000002(N)^{0.222} + 0.042(MC)^{0.616} + 0.00001(DIS)^{0.077}] \quad (8)$$

5. Evaluation of PPV Prediction Models

To evaluate and compare the models in two stages of training and testing, statistical indices including the coefficient of determination (R^2) in equation (9), the root mean square error (RMSE) in equation (10), and the mean absolute percentage error (MAPE) in equation (11) were utilized. In these equations, Y_{meas} and Y_{pred} represent the measured and predicted values, respectively, and represent the calculated $\overline{Y}_{meas}$ and $\overline{Y}_{pred}$ predicted mean values, and n is the number of data.

$$R^2 = 100\left[\frac{\sum_{i=1}^{N}(Y_{meas}-\overline{Y}_{meas})(Y_{pred}-\overline{Y}_{Pred})}{\sqrt{\sum_{i=1}^{N}(Y_{meas}-\overline{Y}_{meas})^2\,(\sum_{i=1}^{N}Y_{pred}-\overline{Y}_{pred})^2}}\right] \quad (9)$$

$$RMSE = \sqrt{\frac{\sum_{i=1}^{n}\left(Y_{meas}-Y_{pred}\right)^2}{n}} \quad (10)$$

$$MAPE = \frac{\sum_{i=1}^{n}\frac{\left|Y_{meas}-Y_{pred}\right|}{Y_{meas}}}{n}\times 100 \quad (11)$$

6. Prediction Performance Evaluation of Statistical Models

In this research, the prediction of PPV was carried out using multivariate linear and nonlinear statistical models. To evaluate and assess the performance of the tested models and determine the best model for optimizing the blast pattern to minimize PPV, equations (9 to 11) were employed. Table 4 presents the evaluation metrics of the models in the training and testing stages. According to the results in this table, the linear regression model exhibits the highest accuracy, while the logarithmic nonlinear regression has the lowest accuracy in predicting PPV. Based on the analysis using the coefficient of determination in both the training and testing phases, Figure 6 illustrates the superiority of the linear statistical model over the other statistical models.

Table 4 Evaluation indicators of training and testing of statistical models

NO	Model	Training			Test		
		R^2	RMSE	MAPE	R^2	RMSE	MAPE
1	Linear regression	0.9247	9.235	12.525	0.8828	6.564	8.806
2	Logarithmic	0.9041	10.663	22.425	0.76	9.813	13.294
3	Exponential	0.8233	19.717	39.68	0.7131	11.091	15.905
4	Polynomial with non-integer coefficients	0.9157	9.732	15.448	0.8578	6.701	9.806

7. Optimizing the Best Statistical Model for PPV Prediction Using the Frog Leaping Algorithm

To optimize the blast pattern for minimizing PPV in the Gol Gohar iron ore mine using the Frog Leaping Algorithm, a need arises for an objective function. To determine the objective function, statistical models are employed. In essence, statistical indicators are responsible for examining and evaluating the objective function, aiming to provide an appropriate model for optimization. Once the objective function is invoked in the Frog Leaping Algorithm, the optimization process begins. The Frog Leaping Optimization Algorithm has a set of control parameters that alter the optimization process when modified. Ultimately, after 25 program executions and 250 repetitions in each run, the final values of these parameters and the optimized blast pattern are obtained, as shown in Tables 5 and 6.

Table 5. Parameters Used in the Frog Leaping Algorithm

Parameters	Symbol	Value
Nvar	Number of decision variables	8
Maximum Number of Iterations	Maxit	250
Number of frogs	Npop	58
Npop Memeplex	Memeplex size	9
Nmemeplex	Memeplex number	5
Attraction value at zero distance	Beta	5
Convergence coefficient	Alpha	3
Absorption coefficient power	Sigma	2

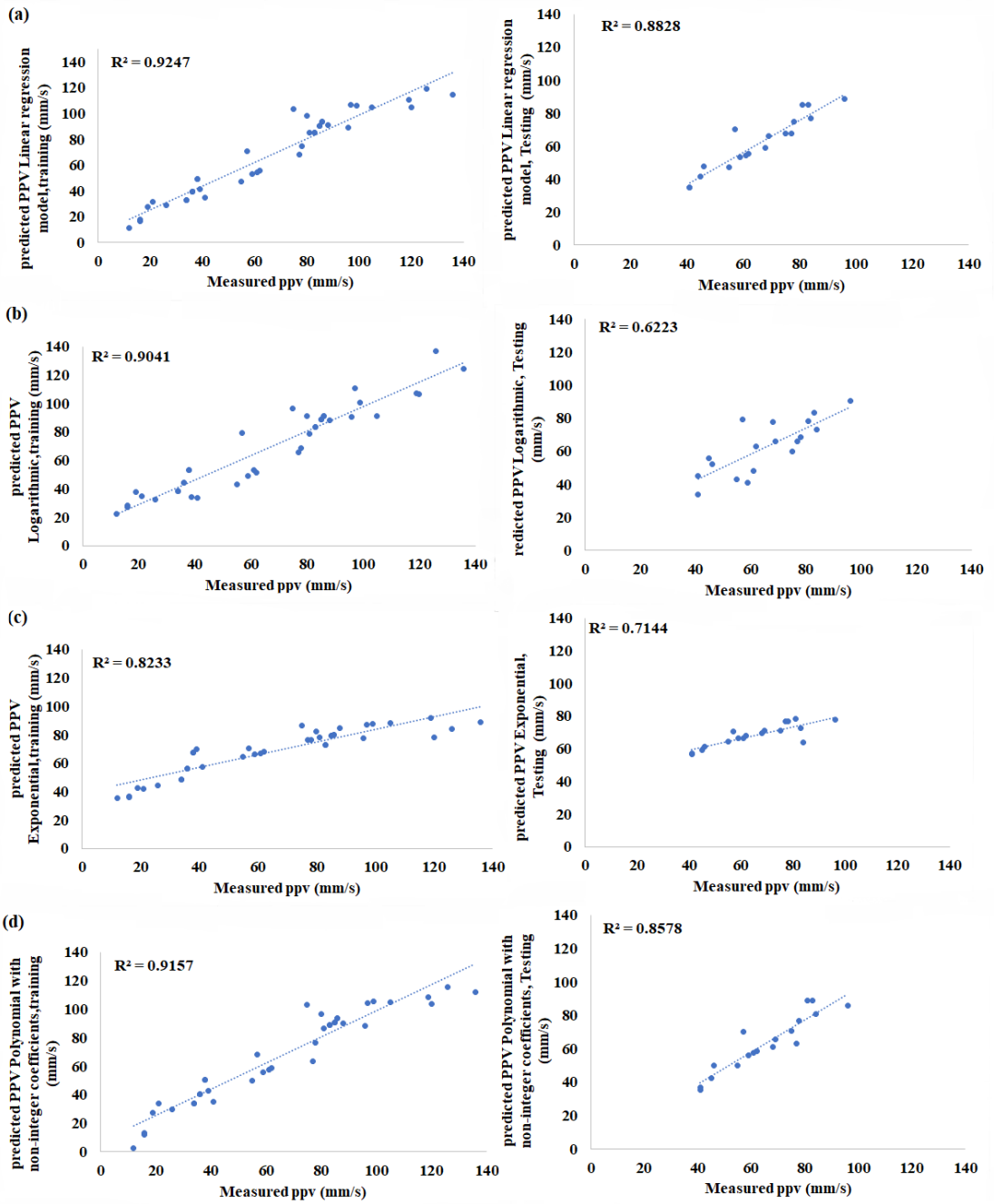

Figure 6. Measured and predicted PPV for training and testing datasets. (a) Using Linear regression, (b) using Logarithmic, (c) using Exponential, (d) using with non-integer coefficients

Table 6. The optimal pattern obtained by the frog algorithm for PPV optimization

No.	Parameter	Symbol	Initial value		Optimized values
			Min.	Max.	
1	Blast hole length (m)	H	6.8	17.5	17
2	Burden (m)	B	2.8	7.5	5.5
3	Spacing (m)	S	4	9.5	7
4	Stemming (m)	ST	2.5	6	5
5	No. of holes	N	21	77	38
6	Total charge (kg)	MC	6400	32250	27629
7	Distance (m)	DIS	62	188	165
8	Maximum velocity (mm/s)	PPV	12	136	59

Certainly, as seen in Table (4), the number of frogs (npop) represents the count of blast patterns collected during the execution of this research. After determining the values of the control parameters for the frog algorithm, the optimization process was carried out over 250 iterations to minimize the PPV. Figure (7) shows the convergence of the optimal solution of the frog algorithm. The best objective function result is displayed after 250 iterations, with the optimal pattern achieving the best result at iteration 50, where PPV is 59

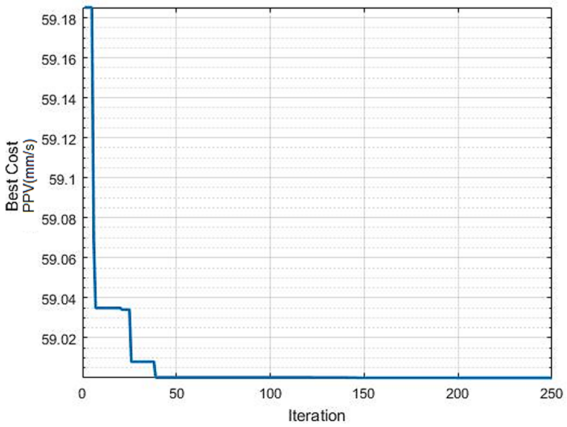

Figure 7. Convergence of the objective function result by the frog algorithm for optimizing PPV

8. Conclusions

Blasting operations, in addition to achieving suitable rock fragmentation, can have various negative and undesirable effects on the environment. If these consequences are not well-controlled, they can lead to significant human and financial damages. Among these effects, ground vibration is one of the most undesirable outcomes of blasting operations. In this study, linear and nonlinear statistical models were developed to predict Peak Particle Velocity (PPV). To enhance and evaluate the models, 58 sets of data collected from Golgohar Iron Ore Mine No. 1 were used, including parameters such as blast hole length, burden thickness, row spacing of blast holes, stemming length, number of blast holes, total explosive charge, and the distance from the seismograph to the blast site.

1) Out of the 58 data sets, forty (40), constituting 80% of the total blasting data, were used for building and training various prediction models, while 18 data samples (20%) were used to evaluate the predictive capabilities of the developed models.

2) To compare the models and identify the best one, several performance evaluation indices were used, including the coefficient of determination (R^2), root mean square error (RMSE), and mean absolute percentage error (MAPE).

(3) Based on the results, the multivariate linear statistical model with values of R^2 = 0.9247, RMSE = 9.235, and MAPE = 12.525 demonstrated superior predictive capability compared to nonlinear statistical models and can be utilized for predicting vibration caused by blasting in the mining industry.

4) Finally, after identifying the best predictive model, a combination of the statistical model and the frog-leaping algorithm was employed to improve model performance and provide an optimal blasting pattern to reduce PPV.

5) Based on the findings, the combination of the statistical model and the frog-leaping algorithm proved to be a robust method for minimizing PPV in blasting operations. The optimized blasting pattern specifications are: blast hole length of 17 (m), burden 5.5 (m), spacing 7 (m), stemming length 5 (m), number of blast holes 38, total explosive charge of 27,629 kg, and seismograph distance from the blast site of 165 (m). The results indicate that using the proposed optimized pattern can reduce PPV by 31%.

References

[1]. Armaghani, D.J., Hajihassani, M., Mohamad, E.T., Marto, A., & Noorani, S. (2014). Blasting-induced flyrock and ground vibration prediction through an expert artificial neural network based on particle swarm optimization. *Arabian J. Geosci, 1(12)*, 1396-1373.

[2]. Amini, H., Gholami, R., Monjezi, M., Torabi, S.R., & Zadhesh, J. (2012). Evaluation of flyrock phenomenon due to blasting operation by support vector machine. *Neural Comput Appl, 21(8)*, 2077-2085.

[3]. Yan,Y., Hou, X., & Fei, H. (2020). Review of predicting the blast-induced ground vibrations to reduce impacts on ambient urban communities. *J Clean Prod*, 260, 121-135.

[4]. Arthur, C.K., Temeng, V.A., & Ziggah, Y.Y. (2020). Novel approach to predicting blast-induced ground vibration using Gaussian process regression. *Eng Comput, 36(1)*, 29-42.

[5]. Li, G., Kumar, D., Samui, P., Nikafshan Rad, H., Roy, B., & Hasanipanah, M. (2020). Developing a new computational intelligence approach for approximating the blast-induced ground vibration. *Applied Sciences, 10(2),* 434.

[6]. Khandelwal, M., & Singh, T.N. (2009). Prediction of blast-induced ground vibration using artificial neural network. *J Rock Mech Min Sci, 46*,1214-1222.

[7]. Singh, P.K., & Roy, M.P. (2010). Damage to surface structures due to blast vibration. *J Rock Mech Min Sci, 47(6)*, 949–961.

[8]. Dehghani, H., & Ataee-pour, M. (2011). Development of a model to predict peak particle velocity in blasting operation. *J Rock Mech Min Sci, 48(1)*, 51–58.

[9]. Monjezi, M., Ghafurikalajahi, M., & Bahrami, A. (2011). Prediction of blast-induced ground vibration using artificial neural networks. *Tunnelling andUnderground Space Technology, 26(1)*, 46–50.

[10]. Hasanipanah, M., Faradonbeh, R.S., Amnieh, H.B., Armaghani, D. J., & Monjezi, M. (2017). Forecasting blast-induced ground vibration developing a CART model. *Eng Comput, 33(2),* 307–316.

[11]. Faradonbeh, R.S., & Monjezi, M. (2017). Prediction and minimization of blast-induced ground vibration using two robust meta-heuristic algorithms. *Eng Comput, 33*, 835–851.

[12]. Ragam, P., & Nimaje, D. S. (2018). Evaluation and prediction of blast-induced peak particle velocity using artificial neural network: A case study. *Noise and Vibration Worldwide, 43(3)*, 111-119.

[13]. Ataei, M., & Sereshki, F. (2017). Improved prediction of blast-induced vibrations in limestone mines using Genetic Algorithm. *J M E, 8(2),* 291-304.

[14]. Agrawal, H., & Mishra, A. K. (2020). An innovative technique of simplified signature hole analysis for prediction of blastinducedground vibration of multi-hole/production blast: an empirical analysis. *Nat Hazards, 100*, 111–132.

[15]. Ainalis, D., Kaufmann, O., Tshibangu, J. P., Verlinden, O., & Kouroussis, G. (2017). Modelling the source of blasting for the numerical simulation of blast-induced ground vibrations: a review. *J Rock Mech Min Sci, 50(1)*, 171–193.

[16]. Gorai, A.K., Himanshu, V.K., & Santi, C. (2021). Development of ANNbased universal predictor for prediction of blast-induced vibration indicators and its performance comparison with existing empirical models. *Min Metall Explor, 38*, 2021–2036.

[17]. Hasanipanah, M., Monjezi, M., Shahnazar, A., Armaghani, D. J., & Farazmand, A. (2015). Feasibility of indirect determination of blast induced ground vibration based on support vector machine. *Measurement, 75*, 289–297.

[18]. Himanshu, V.K., Mishra, A.K., Vishwakarma, A.K., Roy, M.P., & Singh, P.K. (2022). Explicit dynamics based numerical simulation approach for assessment of impact of relief hole on blast induced deformation pattern in an underground face blast. *Geomech Geophys Geo Energy Ge Resour, 8,* 19.

[19]. Himanshu, V.K., Mishra, A.K., Roy, M.P., Vishwakarma, A.K., & Singh, P.K. (2021). Numerical simulation based approach for assessment of blast induced deformation pattern in slot raise excavation. *Int J Rock Mech Min Sci, 144,* 104816.

[20]. Himanshu, V. K., & Roy, M. P. (2017). Prediction of blast induced vibration using numerical simulation. Chapter in Edited book entitled Sustainable Mining Practices*, (ISBN10 8184876041),* 219–227.

[21]. Kumar, S., Choudhary, B.S., & Mishra, A.K. (2022). Modelling the effects of ground vibrations on the surface due to blasting in underground coal mines. *Nat Hazards, 110,* 315–323.

[22]. Kumar, S., Mishra, A.K., Choudhary, B.S., Sinha, R.K., Deepak, D., & Agrawal, H. (2020). Prediction of ground vibration induced due to single hole blast using explicit dynamics. *Min Metall Explor, 37*, 733–741.

[23]. Li, X .P., Huang, J., Luo, Y., Dong, Q., Li, Y. H., Wan, Y., & Liu, T. T.(2017). Numerical simulation of blast vibration and crack forming effect of rock-anchored beam excavation in deep underground caverns. Shock and Vibration, *Article ID 1812080*.

[24]. Monjezi, M., Ahmadi, M., Sheikhan, M., Bahrami, A., & Salimi, A.R. (2010). Predicting blast-induced ground vibration using various types of neural networks. *Soil Dynamics and Earthquake Engineering , 30(11),* 1233-1236 .

[25]. Tian, E., Zhang, J., Tehrani, M. S., Surendar, A., & Ibatova, A. Z. (2019). Development of GA-based models for simulating the ground vibration in mine blasting. *Eng Comput, 35(3),* 849 855.

[26]. Verma, A.K., & Singh, T.N. (2011). Intelligent systems for ground vibration measurement: a comparative study. *Eng Comput, 27(3),* 225– 233.

[27]. Zhang, X., Nguyen, H., Bui, X.N., Tran, Q.H., Nguyen, D.A., Bui, D.T., & Moayedi, H. (2020). Novel soft computing model for predicting blast-induced ground vibration in open-pit mines based on particle swarm optimization and XGBoost. *Natural Resources Research, 29,* 711– 721.

[28]. Zhou, J., Li, C., Koopialipoor, M., Armaghani, D .J., & Pham, B. T. (2021). Development of a new methodology for estimating the amount of PPV in surface mines based on prediction and probabilistic models (GEP-MC). *Int J Min Reclam Environ, 35(1),* 48 68.

[29]. Zhao, S., Wang. L., & Cao, M. (2024). Chaos Game Optimization-HybridizedArtificial Neural Network for Predicting Blast-Induced Ground Vibration. *Appl. Sci, 14*, 3759.

[30]. Fissha,Y., Ikeda, H., Toriya, H., Adachi, T., & Kawamura, Y. (2023). Application of Bayesian Neural Network (BNN) for the Prediction of Blast-Induced Ground Vibration. *Appl. Sci, 13,* 3128.

[31]. Guo, J., Zhao, P., & Li, P. (2023). Prediction and Optimization of Blasting-Induced Ground Vibration in

Open-Pit Mines Using Intelligent Algorithms. *Appl. Sci, 13,* 7166.

[32]. Keshtegar, B., Piri, J., Abdullah, R.A., Hasanipanah, M., Sabri, M.M.S., & Le, BN. (2023). Intelligent ground vibration prediction in surface mines using an ecient soft computing method based on field data. *Front. Public Health, 10.*

[33]. Fissha, Y., Ikeda, H., Toriya, H., Owada, N., Adachi, T., & Kawamura, Y. (2023). Evaluation and Prediction of Blast-Induced Ground Vibrations: A Gaussian Process Regression (GPR) Approach. *Mining. 3,* 659–682.

[34]. Armaghani, D.J., He. B., Mohamad, E.T., Zhang, Y.X., Lai, S.H., & Ye, F. (2023). Applications of Two Neuro-Based Metaheuristic Techniques in Evaluating Ground Vibration Resulting from Tunnel Blasting. *Mathematics. 11,* 106.

[35]. Arthur, C.K., Bhatawdekar, R.M., Mohamad, E.T., Sabri, M.M.S., Bohra, M., Khandelwal, M., & Kwon, S. (2022). Prediction of Blast-Induced Ground Vibration at a Limestone Quarry: An Artificial Intelligence Approach. *Appl. Sci, 12(18),* 9189.

[36]. He, B., Lai, S.H., Mohammed, A.S., Sabri, M.M.S., & Ulrikh, D.V. (2022). Estimation of Blast-Induced Peak Particle Velocity through the Improved Weighted Random Forest Technique. *Appl. Sci, 12,* 5019.

[37]. Lawal, A.I., Kwon, S., Hammed, O.S., & Idris, M.A. (2021). Blast-induced ground vibration prediction in granite quarries: An application of gene expression programming, ANFIS, and sine cosine algorithm optimized ANN. *Int.J.Min. Sci, 31(2),* 265-277.

[38]. Jeluši˘c, P., Ivani˘c, A., & Lubej, S. (2021). Prediction of Blast-Induced Ground Vibration Using an Adaptive Network-Based Fuzzy Inference System. *Appl. Sci, 11,* 203.

[39]. Srivastav, A., Singh Choudhary, B., & Sharma, M. (2021). A Comparative Study of Machine Learning Methods for Prediction of Blast-Induced Ground Vibration. *JME, 12(3),* 667-677.

[40]. Kittikun, P., antachang, K., Thungfung, S., & Petthong, N. (2020). Effect of Blast-induced Ground Vibration on Factor of Safety of Pit Wall Stability. J. Pol. Miner. *Eng. Soc, 1(2).*

[41]. Lawal, A.I., & AdebayoIdris, M. (2020). An artificial neural network-based mathematical model for the prediction of blast-induced ground vibrations*. Int. J. Environ. Stud, 77(2),* 318–334.

[42]. Yu, Z., Shi,X., Zhou, J., Chen, X., & Qiu, X. (2020). Effective Assessment of Blast-Induced Ground Vibration Using an Optimized Random Forest Model Based on a Harris Hawks Optimization Algorithm. *Appl. Sci, 10(4),* 1403.

[43]. Zhang, H., Zhou, J., Armaghani, D.J., Tahir, M.M., Pham, B.T., & Huynh,V.V. (2020). A Combination of Feature Selection and Random Forest Techniques to Solve a Problem Related to Blast-Induced Ground Vibration . *Appl. Sci, 10(3),* 869.

[44]. Mahdiyar, A., Armaghani, D.J., Koopialipoor, M., Hedayat, A., Abdullah, A., & Yahy, Kh. (2020). Practical Risk Assessment of Ground Vibrations Resulting from Blasting, Using Gene Expression Programming and Monte Carlo Simulation Techniques. *Appl. Sci, 10(2),* 472.

[45]. Li, G., Deepak Kumar, D., Pijush Samui, D., Nikafshan Rad, H,. Roy, P., & Hasanipanah, M. (2020) Developing a New Computational Intelligence Approach for Approximating the Blast-Induced Ground Vibration . *Appl. Sci, 10(2),* 434.

[46]. Shakeri, J., Shokri, B., & Dehghani, H. (2020). Prediction of Blast-Induced Ground Vibration Using Gene Expression Programming (GEP), Artificial Neural Networks (ANNs), and Linear Multivariate Regression (LMR). *Arch. Min. Sci, 65(2),* 317-335.

[47]. Mohammadi, D., Mikaeil, R., & Abdollahei Sharif, J. (2020). Investigating and Ranking Blasting Patterns to Reduce Ground Vibration using Soft Computing Approaches and MCDM Technique. *JME, 113,* 881-897.

[48]. Ragama, P., & Nimaje, D.S. (2018). Assessment of Blast-induced Ground Vibration using Different Predictor Approaches- A Comparison. *Chem. Eng. Trans, 66,* 487-492.

[49]. Sirjani, A. K., Sereshki, F., Ataei, M., & Hosseini, M. A. (2022). Prediction of Backbreak in the Blasting Operations using Artificial Neural Network (ANN) Model and Statistical Models (Case study: Gole-Gohar Iron Ore Mine No. 1). *A M S, 67(1),* 107–121.

[50]. Caffo, B. (2019). Regression Models for Data Science in R: A companion book for the Coursera Regression Models class. *Leanpub.*

[51]. Eusuff, M .M., & Lansey, K. E. (2003). Optimization of Water Distribution Network Design Using the Shuffled Frog Leaping Algorithm. *J Water Resour Plan Manag, 129(3),* 210–225.

[52]. Luo, J., & Chen, M. R. (2014). Improved shuffled frog leaping algorithm and its multi-phase model for multidepot vehicle routing problem. *Expert Syst Appl, 41(5),* 2535-2545.

[53]. Kennedy, J., & Eberhart, R. (1995). Particle swarm optimization (PSO). *InProc. IEEE International Conference on Neural Networks, Perth, Australia, 1942-1948.*

[54]. Liping, Z., Weiwei, W., Yi, H., Yefeng, X., & Yixian, C. (2012). Application of shuffled frog leaping algorithm to an uncapacitated SLLS problem. *AASRI Procedia, 1,* 226-231.

[55]. Huynh, T. H. (2008). A Modified Shuffled Frog Leaping Algorithm for Optimal Tuning of Multivariable PID Controllers. *ICIT IEEE Industrial Technology.*

[56]. Ebrahimi, J., Hosseinian, S. H., & Gharehpetian, B. G. (2011). Unit commitment problem solution using shuffled frog leaping algorithm. *IEEE Trans Power Syst, 26(2),* 573-581.

[57]. Jaafari, A., Zenner, E.K., Panahi, M., & Shahabi, H. (2019). Hybrid artificial intelligence models based on a neuro-fuzzy system and metaheuristic optimization algorithms for spatial prediction of wildfire probability. *Agric For Meteorol, 266-267,*198-207.

[58]. Niknam, T., & Farsani, E. A. (2010). A hybrid self-adaptive particle swarm optimization and modified shuffled frog leaping algorithm for distribution feeder reconfiguration. *Eng Appl Artif Intell, 23(8),* 1340-1349.

مطالعه پیش بینی و بهینه سازی لرزش زمین ناشی از انفجار با استفاده از ترکیب مدل آماری و الگوریتم قورباغه موردی: معدن سنگ آهن شماره یک گل‌گهر

عباس خواجوئی سیرجانی[1*]، فرسنگ سرشکی[2]، محمد عطائی[2]، محمد امیری حسینی[3]

۱. دانشکده مهندسی معدن، نفت و ژئوفیزیک، دانشگاه صنعتی شاهرود، شاهرود، ایران
۲. رئیس، بخش معدن و زمین‌شناسی، مدیریت تحقیقات و فناوری گل‌گهر، سیرجان، ایران

ارسال ۲۰۲۴/۰۷/۰۹، پذیرش ۲۰۲۴/۱۱/۱۸

* نویسنده مسئول مکاتبات: abbas3457@gmail.com

چکیده:

مهم‌ترین پیامد مخرب عملیات آتشباری، ارتعاش زمین است. این پدیده نه تنها باعث ناپایداری دیواره‌های معدن می‌شود، بلکه اثرات تخریبی خود را تا چندین کیلومتر بر روی تأسیسات و سازه‌های مختلف نیز گسترش می‌دهد. محققان مختلف برای پیش‌بینی حداکثرسرعت ذرات PPV معادلاتی پیشنهاد کرده‌اند که معمولاً بر اساس دو پارامتر تنظیم می‌شوند: مقدار ماده منفجره در هر تأخیر و فاصله تا محل انفجار. با این حال، بر اساس مطالعات مختلف، نتایج عملیات آتشباری تحت تأثیر عوامل متعددی مانند الگوی آتشباری، ویژگی‌های توده سنگ و نوع مواد منفجره استفاده‌شده قرار می‌گیرد. از آنجا که فناوری هوش مصنوعی هنوز به طور کامل در صنعت معدن مورد بررسی قرار نگرفته است، این مطالعه از مدل‌های آماری خطی و غیرخطی برای تخمین PPV در معدن سنگ آهن شماره ۱ گل‌گهر استفاده کرده است. برای دستیابی به این هدف، ۵۸ مجموعه داده از عملیات آتشباری جمع‌آوری و تحلیل شد که شامل پارامترهایی از جمله طول چال انفجاری، ضخامت بار سنگی، فاصله ردیف‌های چال، طول ساقه‌گذاری، تعداد چال‌ها، مقدار کل ماده منفجره، فاصله لرزه‌نگار از محل انفجار و PPV ثبت‌شده ، سیستم انفجاری با استفاده از فتیله انفجاری بود. در مرحله اول، ارتعاش زمین با استفاده از مدل‌های آماری خطی و غیرخطی چندمتغیره پیش‌بینی شد. در مرحله دوم، به‌منظور تعیین تابع هدف برای بهینه‌سازی طراحی الگوآتشباری با استفاده از الگوریتم جهش قورباغه‌ای ترکیب‌شده، عملکرد مدل‌های آماری با شاخص‌های R^2، RMSE و MAPE ارزیابی گردید. مدل آماری خطی چندمتغیره با مقادیر $R^2 = 0.9247$، $RMSE = 9.235$ و $MAPE = 12.525$ به‌عنوان تابع هدف پیشنهاد و استفاده شد. در نهایت، نتایج نشان داد که ترکیب تکنیک مدل آماری با الگوریتم جهش قورباغه‌ای مرتب‌شده می‌تواند PPV را تا ۳۱٪ کاهش دهد.

کلمات کلیدی: انفجار، لرزش زمین ، مدل‌های آماری، الگوریتم قورباغه، معدن گل‌گهر.